

Synthesis, Characterization and Electrochemical Evaluation of Polyvinylalcohol/Graphene Oxide/Silver Nanocomposites for Glucose Biosensing Application

Seyed Morteza Naghib^{1,*}, Ehsan Parnian², Hamid Keshvari², Eskandar Omidinia^{3,*},
Mahdi Eshghan-Malek¹

¹ Nanotechnology Department, School of New Technologies, Iran University of Science and Technology (IUST), P.O. Box 16846-13114, Tehran, Iran.

² Department of Biomedical Engineering, Amirkabir University of Technology (Tehran Polytechnique), P.O. Box 15875-4413, Tehran, Iran.

³ Enzyme Technology Lab., Genetics & Metabolism Research Group, Pasteur Institute of Iran, P.O. Box 13164, Tehran, Iran.

*E-mail: naghib@iust.ac.ir, skandar@pasteur.ac.ir

Received: 26 September 2017 / *Accepted:* 20 November 2017 / *Published:* 16 December 2017

Hybridization of nanoscale metals and carbon nanostructures into composite nanomaterials has produced some of the best-performing super capacitors and biosensors to date. The challenge remains to develop scalable nanofabrication methods that are amenable to the development of biosensors. A scalable nanostructured composite based on graphene oxide nanosheets (GO), Ag nanoparticles, and a biorecognition element (glucose oxidase) was presented. In addition to good conductivity and biocompatibility, this matrix had a low total cost. The surface of composite was rough due to the presence of GO in PVA matrix that could increase contact area between composite and enzyme layer and consequently enhanced biosensor electrochemical response. Surface morphology was analyzed by SEM and characterization of the composite elements was carried out using FTIR and XRD. Finally, impedance of different samples was determined by electrochemical impedance spectroscopy (EIS) and the effect of GO amount on impedance of the composite was investigated. This method to synthesis of the nanocomposite was devoted to glucose sensing succeeded a favorable device design that also exhibited remarkable glucose biosensing performance such as improved glucose sensitivity (25 nM limit of detection, 15.32 $\text{mAM}^{-1}\text{cm}^{-2}$ of sensitivity, 150 nM to 10 mM of linear range), and excellent selectivity. To the best our knowledge, this device is the first biosensor protocol that used the nanocomposite for glucose determination.

Keywords: nanocomposite, graphene oxide, polyvinylalcohol, biorecognition element, FTIR, XRD

1. INTRODUCTION

Recently, consideration of smart devices and those fields prepare its requirements that has been increased dramatically.

Since these prepared biosensors are attractive due to the widespread use of them in smart materials, extensive studies have been performed on the subject [1-5]. In addition of applications in smart devices, nowadays these diagnostic tools have been used in early and specified diagnosis and monitoring the patients' conditions [6-14].

Use of graphene-based materials in electrochemical biosensors which are the most common biosensors and especially enzymatic ones, is dramatically increasing [9, 15-17]. It is due to the unique properties of graphene and its compatibility with sensing applications. Graphene oxide nanosheets can be considered as acceptable medium between biological diagnostic elements and electron transferring components because of their special planar configuration, good conductivity, and high electrocatalytic activity [17-21].

Chan et al. casted 60 μL graphene oxide solution (0.5 mg/mL) on a gold plate and reduced it at 65°C by adding hydrazine overnight to prepare a biosensor for ultrasensitive detection of enzymatic activity. This graphene-based substrate was used to immobilize and detect the activity of SNAP-25-GFP peptide complex [22]. In another study, Shen-Ming Chen et al. prepared a composite of graphene oxide-Ag nanoparticles solution (1 mL of graphene oxide solution 0.5 mg/mL and 2 mL of AgNO_3 solution 0.5 mM) and then reduced graphene oxide by performing 20 successive cyclic voltammograms from 0 to -1.4 V at the scan rate of 50 mV/s [23]. Yang et al. prepared graphene oxide according to the modified hummer's method [24] by the exfoliation of graphite. Then, resultant graphene oxide was coupled to SDBS by ultrasonic treatment for 2 h. Then graphene oxide reduced with 30 μL hydrazine at 100°C for 24 h and the color of the solution changed from yellow brown to black after reduction of GO [25].

At present, various approaches have been developed for the fabrication of graphene-based materials. Solution method is one of the simplest and cheapest approaches [23]. This method also can be used in pilot and industrial scales and since these biosensors are disposable and simple requirements for creation of thin films on the working electrode surface, this method is a suitable choice. So in this study, a composite was prepared using solution method that Poly vinyl alcohol (PVA) as a biocompatible matrix to improve enzymatic stability and activity, Ag nanoparticles for enhancing conductivity and graphene oxide as main component to create electroactivity properties.

The use of PVA in biosensors is very common because of its proper biocompatibility in exposing to enzymes and antibodies, anti-microbial properties, high thermal stability, desirable physical properties such as good film forming property, elastic nature, and high degree of swelling in aqueous solutions [26, 27]. Although PVA membrane has been employed in construction of glucose [26], triglyceride (TG) [27], ethanol [28], polyphenol [29], L-phenylalanine [14] and some other biosensors, its application for other biosensors has not been reported so far.

It has been proved that Ag is the best conductive materials among metals [30, 31]. Thus Ag nanoparticles have a better conductivity than Au nanoparticles in biosensors. In this work, Ag

nanoparticles has been used as an electron transfer facilitator due to its good electrocatalytic response [32] to enhance the biosensor sensitivity.

In previous studies established in order to achieve an appropriate matrix for immobilization of enzymes that detected glucose amount, generally carbon-based material and an additive were used. Sarkar et al. used a carbon matrix with 5% rhodium to immobilize various amino acid oxidizing enzymes. Rhodium has been added to enhance hydrogen peroxide sensing [33].

Stefan-van Staden et al. developed a diamond paste containing amino acid oxidizing enzymes to determine L- and D-Enantiomers of leucine [34]. In another study by Rezaei et al., a modified glassy carbon electrode with multiwall carbon nanotubes was used to measure leucine level in biological samples. They used non-enzymatic method and showed that carbon nanotubes enhanced biosensor sensitivity [35].

In this study we used a simple and non-expensive method to fabricate a versatile nanocomposite matrix that could play a significant role in achieving a sensitive, specific, and low-cost biosensor that can be used in electrochemical monitoring. For this reason, the nanocomposite was prepared from graphene oxide nanosheets and Ag nanoparticles in PVA matrix. In addition to good conductivity and biocompatibility, this matrix had a low total cost. The surface of the nanocomposite was rough due to the presence of GO in PVA matrix that could increase contact area between the composite and enzyme layer and consequently enhanced biosensor electrochemical response. Surface morphology was examined by SEM and characterization of composite elements was performed using FTIR and XRD. Finally, impedance evaluation of different samples was established by electrochemical impedance spectroscopy (EIS) and the effect of GO amount on impedance of the composite was investigated. Then, the enzyme, glucose oxidase, was immobilized onto the nanocomposite surface via a simple approach and biosensing performance of the enzyme electrode was evaluated.

2. MATERIALS AND METHOD

2.1. Reagents and equipment

Silver nitrate (biochemical grade) and poly (vinyl alcohol) (PVA, 96% hydrolyzed, MW 72 kDA) were purchased from Merck (Germany). GO nanoplatelets (99.5+%, 2-18 nm with 32 layers) were prepared from US Nano (USA). All chemicals were used as received and prepared using distilled water.

Attenuated total reflection fourier transform infrared spectroscopy (ATR FT-IR) spectra was recorded on a Nexus 670 (Thermo Nicolet, USA) using ZnSe 45° discs. The morphology of the nanobiocomposite samples was measured using a Sigma field emission electron microscope (FESEM) (Zeiss, Germany) operated at 25 kV. For imaging, 4 samples were synthesized on glass slides and coated by a thin Au layer. Also energy dispersive spectroscopy (EDS) (Oxford Instruments, England) was used to determine elemental weight percentages.

2.2. Synthesis of the nanocomposite

As shown in Fig. 1, PVA solution (2.5 mg/mL) was prepared by adding PVA powder to distilled water while mixing on magnetic stirrer at 60 °C. GO dispersion (2.5 mg/mL) was prepared by adding graphene oxide nanosheets powder to distilled water and the dispersion was homogenized by a vortex for 1 min. To prepare 0.5 mM AgNO₃ aqueous solution, 850 mg AgNO₃ powder was mixed with 10 mL distilled water and then fully mixed by magnetic stirrer.

To prepare PVA/GO/Ag nanoparticles composite solution, 200 µL of GO solution was mixed with 400 µL of AgNO₃ aqueous solution and homogenized by a vortex for 1 min. The obtained mixture of AgNO₃ and GO (2:1 ratio) was ultrasonicated using a Sonorex Digitec DT-100 bath sonicator (Bandelin, Germany) at room temperature for 15 min to obtain a stable aqueous dispersion. After sonication, the color of dispersion changed to light gray. Finally, 600 µL of obtained GO-Ag solution was gradually added to 600 µL PVA solution while the solution was mixing by magnetic stirrer and then fully mixed by stirrer for 5 min.

10 µL of PVA/GO/Ag NPs solution was casted on a glassy slide and allowed to dry at room temperature to form composite and used as sample for subsequent characterizations. All experiments were carried out at room temperature (25 ± 1 °C) and standard conditions. Other samples were prepared with the same method except ratios of the components listed in Table 1.

Table 1. Components ratios of samples used to investigate composite properties. (All values reported in µL).

sample number	PVA solution	GO solution	AgNO ₃ solution	Glucose oxidase	distilled water
1	600	-	-	-	600
2	600	-	400	-	200
3	600	200	-	-	400
4	600	200	400	-	-
5	600	200	400	10	-

2.3. Preparation of working electrode and enzyme containing sample

Five different samples were examined for conductivity, electrochemical and sensory responses to study the effect of each component. To prepare samples 1 to 4, 8 µL of related solution was casted on a gold working electrode and allowed to dry at room temperature for 24 h to form composite. The Au working electrode was connected to an autolab PGSTAT 30 (Echo chemie, B.V., Netherlands), potentiostat/galvanostat connected to a three electrode cell, Model 6.1414.010 stand (Metrohm, Switzerland) linked with a computer (Pentium IV, 1200 MHz) and NOVA software (version 1.7.8). Sample 5 was prepared by the same method and after forming the composite, 6 µL of glucose oxidase was casted on the composite layer and kept at 4 °C (in a refrigerator) for 24 h and then was washed carefully to obtain a suitable enzyme electrode.

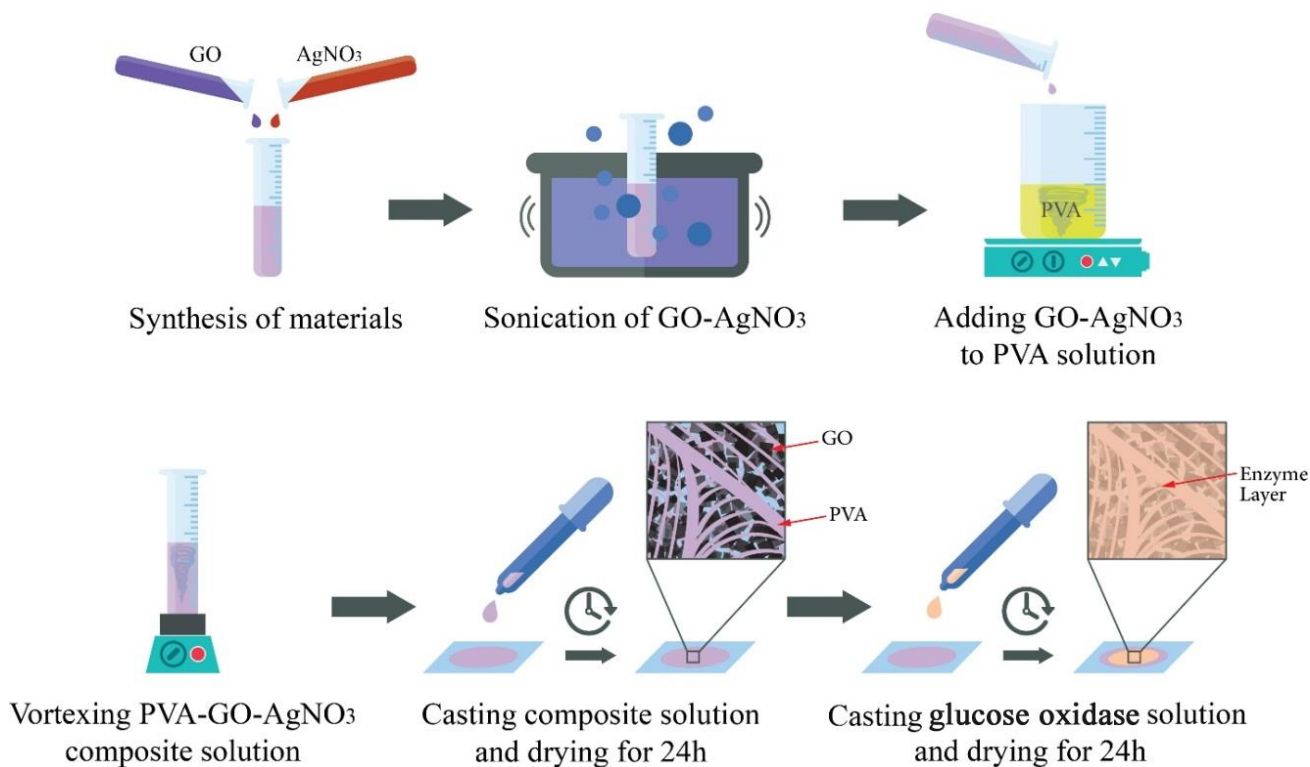


Figure 1. Schematic representation of the bionanocomposite synthesis.

3. RESULTS AND DISCUSSION

3.1. X-ray powder diffraction (XRD) analysis

To study the characteristics of the crystal structure and prove the immobilization of enzyme layer on the composite surface, samples 4 and 5 were analyzed with X-ray powder diffraction (XRD) method. According to Fig. 2a, X-ray diffraction pattern for full composite structure containing PVA, GO and Ag, at angles of 44, 65 and 112 showed clear peaks that further represented the composite stabilization on the surface. In sample 5 that the holder surface coated with enzyme layer after composite consolidation, distinctive peaks were observed at angles of 14, 18, 23, 27, 37, 45, 64 and 112.

By comparing the results of two samples, the differences of the diffraction patterns were determined and immobilization of the enzyme layer was confirmed. According to Fig. 2a, when only composite was immobilized on the surface, no diffraction was observed at angles between 15 to 37, while after enzyme coating on the surface, significant peaks were observed at the angles of 14, 18, 23, 27 and 37 that was relative to the presence of the enzyme layer on the surface. The intensity of peaks observed at angles of 44, 65 and 112 was reduced due to the covering the enzyme layer. This phenomenon reflected the presence of the enzyme as well as composite layer.

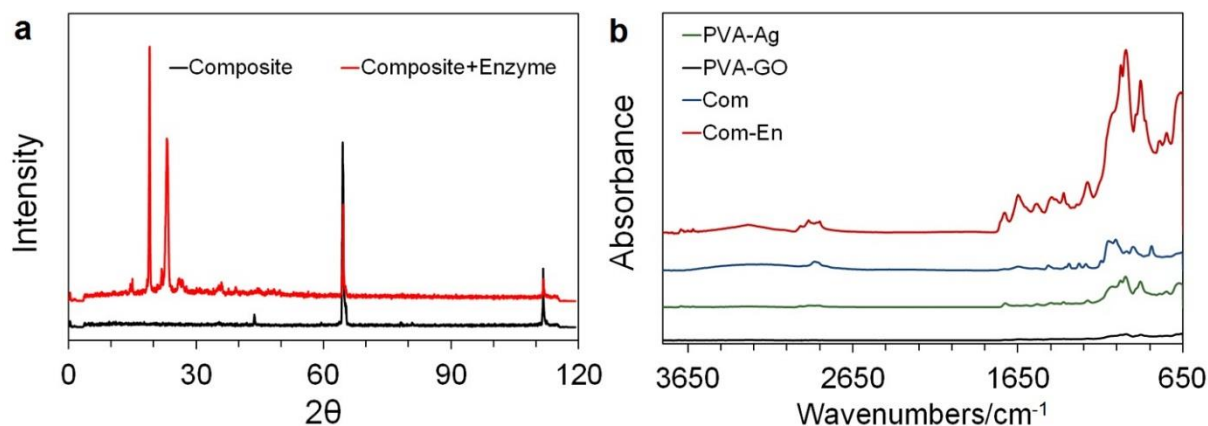


Figure 2. (a) Comparison of XRD results obtained from samples 4 and 5: stabilized composite layer without enzyme layer (black line) and the composite stabilized on the surface coated by the glucose oxidase layer (red line). (b) ATR Spectra of the samples 2 to 5.

3.2. ATR-FTIR analysis

Composite elements and surface functional groups were characterized by ATR-FTIR. For this purpose, 100 μL of PVA-GO-AgNO₃ solution dropped on aluminum foil and dried for 24 h at room temperature. Sample 5 was prepared with the same method: 10 μL of glucose oxidase enzyme casted on it and dried for another 24 h at room temperature to immobilize the enzyme layer.

According to the results obtained from Fig. 2b, between wavelengths of 650 to 1200 nm, sample 3 showed the minimum absorption. Samples 2 and 4 which respectively contained PVA-Ag and nanocomposite showed close values of absorption. It was due to higher absorption of metallic Ag nanoparticles compared to GO nanosheets. Ag portion was more effective on absorption and spectrum of the composite that was almost dependent on Ag concentration. Finally, sample 5 showed the most absorption among all samples due to the existence of enzyme layer and this result approved the proper coating of biological elements on the composite layer. Moreover, this sample showed significant peaks between 1200 to 1800 nm that was due to the existence of the enzyme layer.

Resulting peaks in the final composite sample showed the existing groups in the composite such as alkenes, graphene oxide rings and alcoholic groups of PVA. Sample containing composite coated with enzyme layer showed the specific functional groups of enzymes like carboxylic acids and amines. Moreover, these results approved the enzyme immobilization on the composite elements.

3.3. FESEM analysis

Surface morphology and elemental analysis were studied using FESEM. As shown in Fig. 3a, sample containing PVA and Ag formed a twisted porous matrix that showed the presence and formation of polymeric layer.

In sample containing PVA and GO, GO sheets were distributed between polymeric matrix, so a rough surface was formed (Fig. 3b). As illustrated in resulting images, GO sheets were well distributed in polymer matrix and edges were protruded from the surface that made a good roughness for more

contact area and better electron transfer (Fig. 5). It was due to the conductivity of GO and groups that located on edges of sheets which start electron transfer process.

Image of sample 4 containing PVA-GO-Ag (Fig. 3c) showed a jagged disordered pattern on the surface. It was because of co-existence of Ag ions and GO sheets. Therefore, a matrix of PVA with small areas of GO sheets and Ag were formed. Thus, the final substrate for the enzyme immobilization had significant roughness that could cause to more contact area between composite as biosensor transducer and enzyme as biological element. Also, PVA matrix enhanced the enzyme biocompatibility.

Vertical alignment of GO sheets relative to the PVA matrix increased the contact area between enzyme and GO and hence significantly enhanced the electron transfer. According to the images, aggregation of Ag in contact to GO was another reason for enhancing conductivity. However, co-existence of Ag and GO in PVA matrix formed many pores on the surface. Due to the penetration of the enzyme solution in these pores before drying, good stability and contact of enzyme layer were established.

In sample 5 (Fig. 3d), enzyme layer was fully coated on the composite surface. Some little cavities were formed on the surface of the enzyme layer because of penetration of solution in the composite pores. This layer had a good connection to conductive composite in the bottom surface and the top surface could react with the analyte. Due to the porous surface of the composite, some ups and downs has been formed on the outer surface of the enzyme layer that could increase contact area between biological element and unknown material and consequently enhanced the electrocatalytic response. Some areas were also flat with no ups and downs.

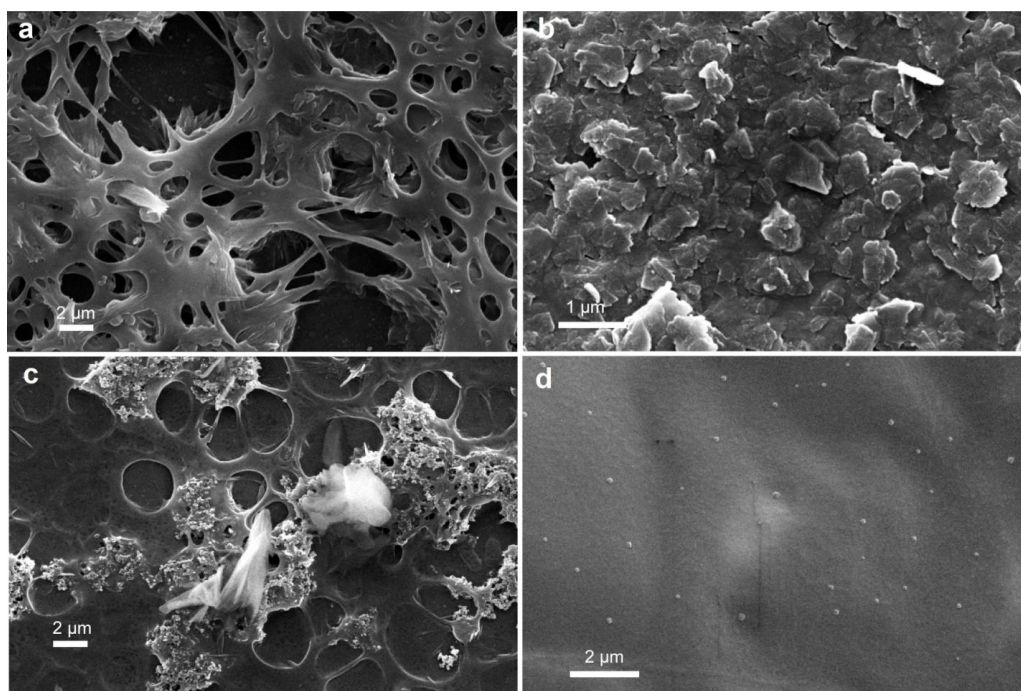


Figure 3. (a) FESEM image of sample 2 (PVA-Ag NPs). (b) FESEM image of sample 3 (PVA-GO nanosheets). (c) FESEM image of sample 4 (PVA-GO-Ag composite). (d) FESEM image of sample 5 (enzyme coated composite).

3.4. EDS analysis

Energy dispersive spectroscopy (EDS) was performed on samples 2 to 5 to determine elemental weight percentages of the composite and to ensure appropriate immobilization. According to the results, sample 2 had a high weight percentage of carbon and oxygen which was due to the presence of PVA (Fig. 4b). These ratios of elements indicated the presence of carbon and oxygen in the PVA chain.

Also in sample 3, considerable weight percentage of carbon and oxygen was reported that was due to the presence of GO sheets in this sample (Fig. 4a).

Sample 4 also indicated a lot of oxygen which showed the presence of PVA and graphene oxide sheets (Fig. 4c). A low percentage of Ag was detected which confirmed the presence of silver nanoparticles in the composite.

As expected, in sample 5 a very high percentage of carbon and oxygen was reported and other elements were seen in the previous samples that were not detected in this sample (Fig. 4d). Noteworthy, presence of carbon and oxygen was because of the presence of glucose oxidase layer which was coated on the surface.

As expected, the elements in the composite components demonstrated a high percentage in this characterization and immobilization of the enzyme composite with intended components was confirmed with this method.

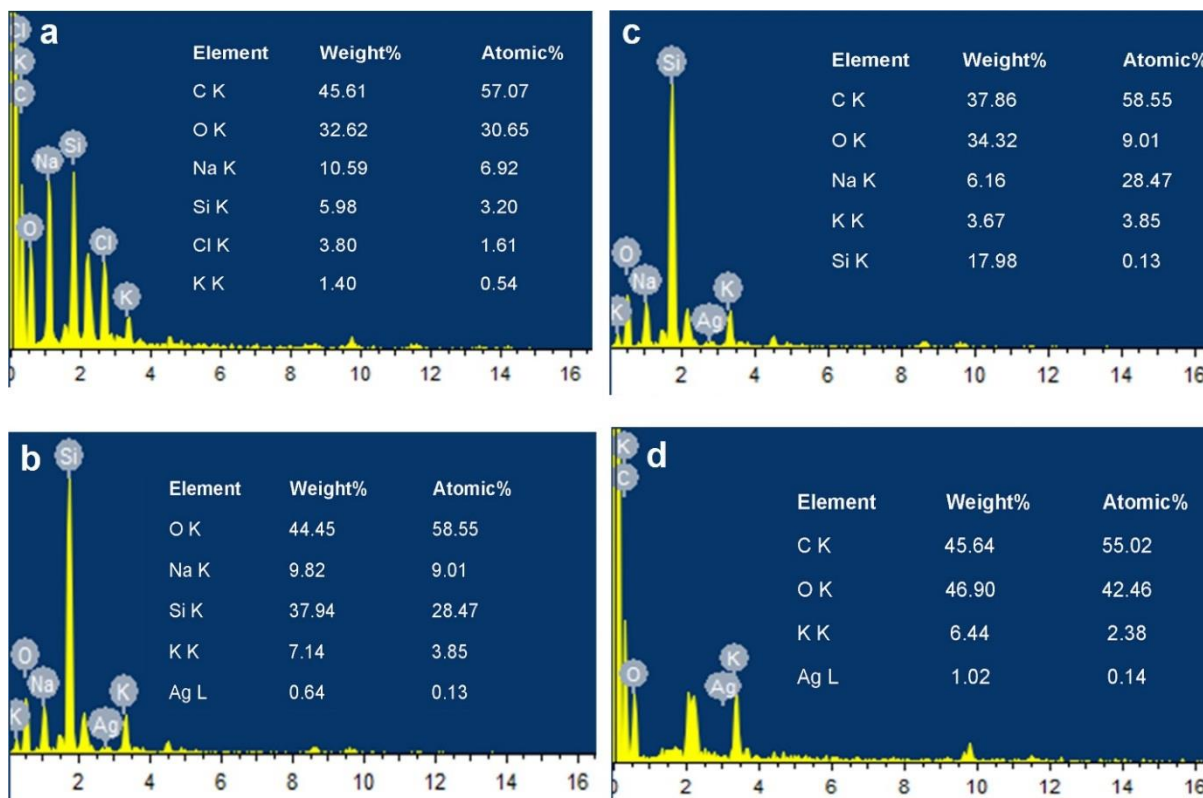


Figure 4. (a) EDS results of sample 3 (PVA-GO). (b) EDS results of sample 2 (PVA-Ag NPs). (c) EDS results of sample 4 (PVA-GO-Ag). (d) EDS results of sample 5 (PVA-GO-Ag-En).

3.5. Cyclic voltammetry and impedance spectroscopy

For the present study, cyclic voltammograms in 0.01 M PBS (pH 7.4) containing 5 mM $K_3Fe(CN)_6$ were applied on FTO electrode for samples 1, 3, 4 and 5. Also in another study for each electrode, Nyquist plots were obtained. The results of this experiment were illustrated in Fig. 5a and Table 2 summarized some important parameters extracted from the Fig. 5. These results indicated that by modifying electrode, conductivity of the electrode was considerably increased and the charge transfer resistance (R_{ct}) was decreased. In Nyquist diagram, the semicircle portion observed at high frequencies corresponded to R_{ct} . This resistance can be directly measured as the semicircle diameter. According to Fig. 5b, there was completely conformity between CV curves and Nyquist plots because with decreasing the R_{ct} , peak height in CV increased and also, the highest charge transfer resistance (R_{ct}) was for PVA coated FTO (~18,000 Ω) and the lowest one (the best) was for the final modification (PVA-GO-AgNPs modified electrode) (~8,000 Ω) which had more impedance reduction than some of the similar previous studies [23]. Zhang et al. investigated an Au electrode modified with gold nanoparticles for use as glucose biosensor. The R_{ct} increased after treatment to 9000 Ω [36]. Iron oxide nanoparticles–chitosan composite based glucose biosensor was fabricated that the total R_{ct} was very high [37]. Similar researches were studied by others that the final R_{ct} was higher than this work [38-40].

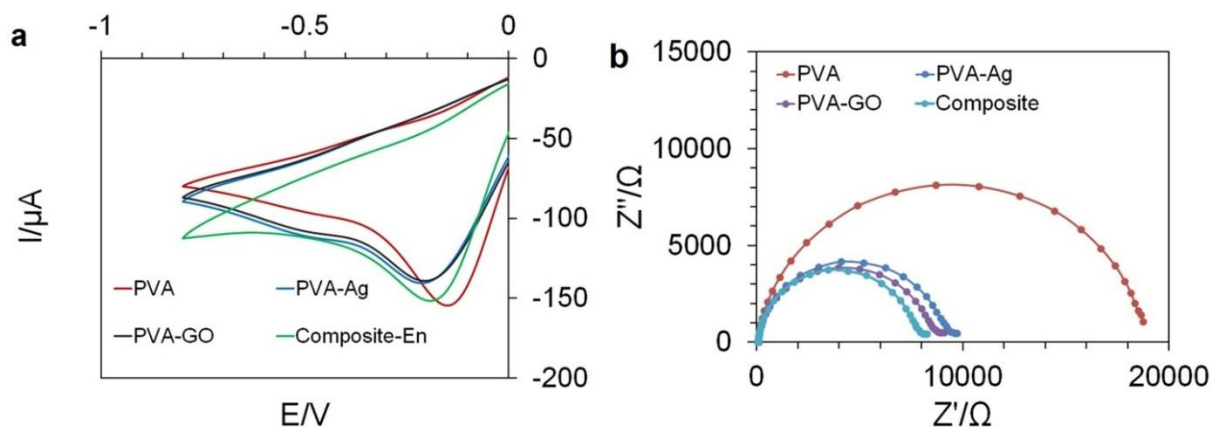


Figure 5. (a) Cyclic voltammetry curve of samples 1 to 5 coated on the electrode at scan rate of 10 mV/s containing 5 mM $K_3Fe(CN)_6$. (b) A comparison of impedance data of the samples 1 to 4.

Table 2. Important parameters of modifying FTO electrode step by step

Working electrode	R_s (Ω)	R_{ct} (Ω)	R_{ctME} / R_{ctBE} (%)
FTO	95	11,000	-
S1	97	17,000	154
S2	96	9,000	81
S3	92	8,000	72
S4	90	7,000	63
S5	-	-	-

3.6. Biosensing activity over glucose determination

Fig. 6 showed biosensing activity of the enzyme electrode to determination of the analyte, glucose. The effect of temperature on the activity of the enzyme electrode was depicted in Fig. 6a. Based on the figure, the optimum temperature for biosensing activity was almost 37°C, demonstrating favorable activity of the biosensor in physiological temperature. A sample current-time followed amperometric response of the modified electrode was observed on the steady addition of the analyte to the cell in the optimized conditions (Fig. 6b). With the increment of the glucose concentration, the biosensor current response was enhanced.

Fig. 6b exhibited a favored linear relationship between the response current and the analyte level (from 150 nM to 10 mM with a correlation coefficient of 0.98). The dynamic amperometric curve developed a remarkable sensitivity equal to $15.32 \text{ mA} \cdot \text{M}^{-1} \cdot \text{cm}^{-2}$ and a limit of detection (LOD) equal to 25 nM (signal-to-noise ratio=3).

According to table 3, the biosensing range and detection limit of the PVA-based biosensor (150nM–10 mM and 0.025 μM) were comparable to or considerably better than that of other graphene or Ag based enzymatic glucose sensors for determining the analyte, glucose, establishing PVA-GO-Ag/glucose oxidase great capacity for diagnosis applications. The great sensitivity of catalytic sensor, the broad linear sensing range and very low detection limit could be related to the nature of Ag-GO [21] based on PVA matrix and thus the existing graphene as a suitable substrate for immobilized enzyme layer which enhanced the electron transfer and moreover electrical conductivity of the biodevice. Moreover, Ag-GO complexes could excellently entrap the PVA matrix and thus could greatly improve the electrocatalytic bioactive areas and increase the direct electron transfer. Furthermore, the enzyme nanocomposites could supply larger active surface area for coupling the substrate, glucose, to the enzyme. Additionally, the superior linear detecting range of the proposed sensor, from 150 nM to 10 mM, was favorable for the further clinical diagnostic applications. It can be seen from structural and sensing characteristics of the nanocomposites that the existence of the porous PVA-based materials caused novel sensing features such as excellent linear sensing range, high sensitivity and very low detection limit than similar materials or substrates (table 3).

Table 3. The comparison of this sensor with other related devices.

Reference	Electrode	Detection limit	Linear range
This sensor	Ag-GO-PVA	25 nM	150 nM-10 mM
[41]	Ag-GO-ZnO-chitosan	10.6 μM	0.1 mM-12 mM
[42]	rGO-Ag	0.16 mM	0.5 mM-12.5 mM
[43]	mesocellular graphene foam	0.25 mM	1 mM-12 mM
[44]	rGO-Ag-titanium dioxide nanotube	2.2 μM	5 mM-15.5 mM
[45]	carbon nanotubes-GO	28 μM	0.05 mM-23.2 mM
[46]	rGO-Au	10 μM	1 mM-8 mM

[47]	graphene	-	0.1 mM-27 mM
[48]	Graphene-polyaniline-Au	0.1 mM	0.2 mM-11.2 mM
[49]	rGO-multiwalled carbon nanotubes	4.7 μ M	0.01 mM-6.5 mM
[50]	Graphene-polyaniline-Au	4 μ M	1 mM-12 mM

Ag-graphene-ZnO-chitosan [41], reduced graphene oxide-Ag [42], mesocellular graphene foam [43], reduced graphene oxide-Ag-titanium dioxide nanotube [44], carbon nanotubes-graphene oxide [45], reduced graphene oxide-Au [46], Graphene-polyaniline-Au [48], reduced graphene oxide-multiwalled carbon nanotubes [49], and Graphene-polyaniline-Au [50] composites were used as a biosensor for glucose sensing that most of their sensing parameters were similar or comparable with this study (table 3).

3.7. Selectivity experiment

Many reagents and active components in biological fluids (such as dopamine, ascorbic acid, amino acids and etc.) could affect adverse reactions. This problem may decrease selectivity and accuracy of the biosensor. Thus, the survey on the influence of possible interfering species on the biosensing activity is very critical. This study aimed to investigate influences of 3.0 mM dopamine, L-phenylalanine, and ascorbic acid as potential interferents (side effects were from 3.25% (max) to 1.03% (min) in maximum reducing or increasing the output current response of the biosensor respectively (Fig. 6c)). Consequently, the sensor proposed that the enzyme electrode had excellent selectivity over electroactive species because of the catalytic enzyme activity of glucose oxidase.

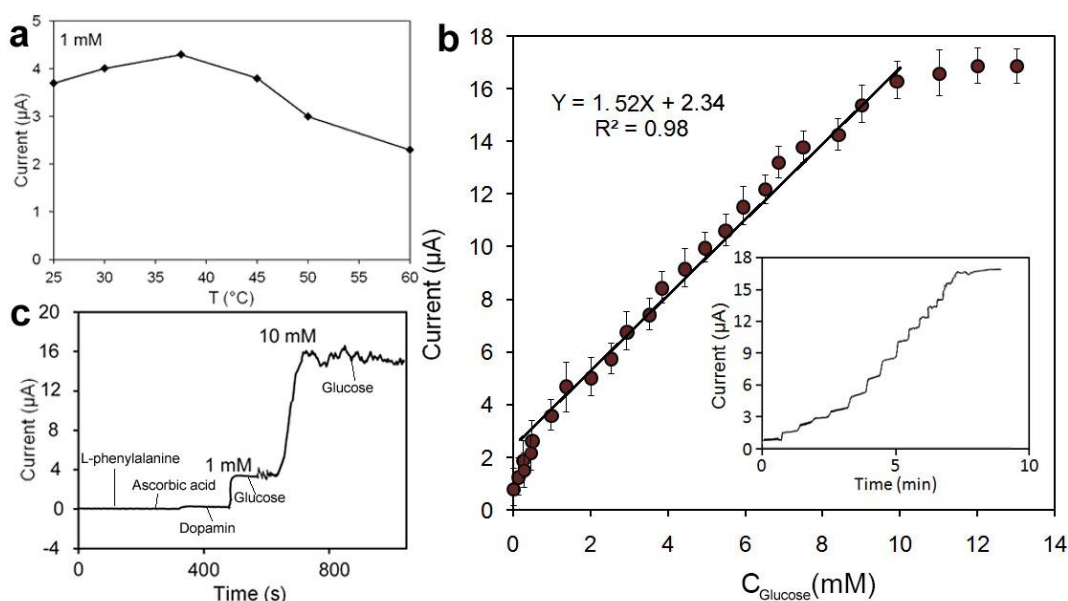


Figure 6. (a) The effect of temperature on the activity of the enzyme electrode. (b) Calibration curve obtained from successive additions of the analyte; the inset shows amperometric response of the biosensor in stirring solution to the successive additions of glucose. (c) The selectivity test of the modified electrode. Initial working volume: 12 mL; supporting electrode: 100 mM phosphate buffer (pH 7.0).

3.8. Human real sample measurements

As well as selectivity tests, the human real sample measurements are essential for deep assessment of biosensors. Thus, the possibility of the new electrochemical biosensor for determination of the analyte, glucose, in real biological sample was studied for more guarantee. The biosensor was applied to detect the analyte level in human blood by the gold standard adding approaches. It is known that the standard dose of glucose level in human blood is $4.5 < C_{\text{glucose}} < 6.5$. The obtained human blood samples were proposed by several normal and patient humans acquired from Tehran University of Medical Sciences. Ten real sample extractions with various analyte doses (from different humans) of 0.5, 1.0, 3.0, and 8.0 mM (tested with a standard method) was evaluated by the biodevice. Table 4 showed the recovery of the current responses of the enzyme electrode. Based on the main results, the recovery output was in the range of 97.32–107.19% and the relative standard deviation (RSD %) was in the range of 1.09–4.2%.

Table 4. Determination and output recovery results of the analyte, glucose, in the real samples using the sensor (N=5)

Samples	The addition content (mM)	The detection content (mM)	RSD (%)	Recovery (%)
Human blood	0.0	0.23	3.1	-
	0.5	0.69	2.26	98.58
	1.0	1.25	1.09	104.17
	3.0	3.43	4.2	107.19
	8.0	7.98	2.87	97.32

4. CONCLUSION

Composite samples for use in transducer of electrochemical biosensors were prepared with solution method. Five samples were prepared using PVA based-material with Ag nanoparticles, GO nanosheets and both (composite and enzyme composite) as well as with an enzyme layer. The resulting composite had set of properties required for the use in transducer of electrochemical biosensors. More specifically, PVA-GO-Ag composite had a good electrical conductivity to transfer electrons, a biocompatible surface for immobilizing biological elements, simple and inexpensive method for preparation and shaping, and also sufficient strength and stability for this application. Based on the results, it was found that simultaneous presence of PVA, GO and Ag nanoparticles minimized the impedance and maximized the electrocatalytic activity of the composite in certain voltage ranges. Thus, obtained composite was favorable material for use in biosensor applications. The developed biosensor demonstrated excellent sensing range with a linear response up to 10 mM with detection limit of 25 nM and also had superior selectivity over interferences. It may be expected that other biomolecules can be combined in the nanocomposites for the designing better sensors.

References

1. C.H. Ahn, J.W. Choi, G. Beaucage, J.H. Nevin, J.B. Lee, A. Puntambekar, J.Y. Lee, *Proceedings of the IEEE*, 92 (2004) 154.
2. B. Das, M. Mandal, A. Upadhyay, P. Chattopadhyay, N. Karak, *Biomed. Mater.*, 8 (2013) 035003.
3. B.K. Gorityala, Z. Lu, M.L. Leow, J. Ma, X.W. Liu, *J. Am. Chem. Soc.*, 134 (2012) 15229.
4. S.M. Naghib, M. Rabiee, E. Omidinia, *Int. J. Electrochem. Sci.*, 9 (2014) 2301.
5. S.M. Naghib, M. Rabiee, E. Omidinia, *Int. J. Electrochem. Sci.*, 9 (2014) 2341.
6. L. Feng, Y. Chen, J. Ren, X. Qu, *Biomaterials.*, 32 (2011) 2930.
7. H. Wang, Y. Yuan, Y. Chai, R. Yuan, *Small.*, 11 (2015) 3703.
8. W.I. Perez, Y. Soto, J.E. Ramirez-Vick, E. Melendez, *J. Electroanal. Chem.*, 751 (2015) 49.
9. X. Kang, J. Wang, H. Wu, I.A. Aksay, J. Liu, Y. Lin, *Biosens. Bioelectron.*, 25 (2009) 901.
10. H. Wang, Y. Bu, W. Dai, K. Li, H. Wang, X. Zuo, *Sensor. Actuat. B-Chem.*, 216 (2015) 298.
11. Z. Wang, Y.Z. Chen, S. Zhang, Z. Zhou, *Conference. Proceedings.*, 2 (2005) 1913.
12. S.M. Naghib, M. Rabiee, E. Omidinia, P. Khoshkenar, *Electroanal.*, 24 (2012) 407.
13. P. Labroo, Y. Cui, *Anal. Bioanal. Chem.*, 406 (2014) 367.
14. S.M. Naghib, M. Rabiee, E. Omidinia, P. Khoshkenara, D. Zeini, *Int. J. Electrochem. Sci.*, 7 (2012) 120.
15. C. Shan, H. Yang, J. Song, D. Han, A. Ivaska, L. Niu, *Anal. Chem.*, 81 (2009) 2378.
16. Z. Wang, X. Zhou, J. Zhang, F. Boey, H. Zhang, *J. Phys. Chem. C.*, 113 (2009) 14071.
17. M. Zhou, Y. Zhai, S. Dong, *Anal. Chem.*, 81 (2009) 5603.
18. R.L. McCreery, *Chem. Rev.*, 108 (2008) 2646.
19. J. Wang, *Electroanal.*, 17 (2005) 7.
20. S.M. Naghib, *Anal. Bioanal. Electrochem.*, 8 (2016) 453.
21. S.M. Naghib, M. Rahmanian, K. Majidzadeh-A, S. Asiaei, O. Vahidi, *Int. J. Electrochem. Sci.*, 11 (2016) 10256.
22. C.Y. Chan, J. Guo, C. Sun, M.K. Tsang, F. Tian, J. Hao, S. Chen, M. Yang, *Sensor. Actuat. B-Chem.*, 220 (2015) 131.
23. S. Palanisamy, C. Karuppiah, S.M. Chen, Colloids and surfaces. B, *Biointerfaces.*, 114 (2014) 164.
24. H.A. Becerril, J. Mao, Z. Liu, R.M. Stoltenberg, Z. Bao, Y. Chen, *ACS. Nano.*, 2 (2008) 463.
25. Y. Yang, A.M. Asiri, D. Du, Y. Lin, *The Analyst.*, 139 (2014) 3055.
26. C.M. Wu, S.A. Yu, S.L. Lin, *Express. Polym. Lett.*, 8 (2014) 565.
27. C.S. Pundir, B. Sandeep Singh, J. Narang, *Clin. Biochem.*, 43 (2010) 467.
28. Y.C. Tsai, J.D. Huang, C.C. Chiu, *Biosens. Bioelectron.*, 22 (2007) 3051.
29. J. Narang, S. Chawla, N. Chauhan, M. Dahiya, C.S. Pundir, *J. Food. Meas. Characterization.*, 7 (2013) 22.
30. C.A. Kraus, *J. Am. Chem. Soc.*, 44 (1922) 1216.
31. E. Omidinia, S.M. Naghib, A. Boughdachi, P. Khoshkenar, D.K. Mills, *Int. J. Electrochem. Sci.*, 10 (2015) 6833.
32. M.J. Song, S.W. Hwang, D. Whang, *J. Appl. Electrochem.*, 40 (2010) 2099.
33. P. Sarkar, I.E. Tothill, S.J. Setford, A.P. Turner, *The Analyst.*, 124 (1999) 865.
34. R.L. Stefan-van Staden, L. Shirley Muvhulawa, *Instr. Sci. Technol.*, 34 (2006) 475.
35. B. Rezaei, Z.M. Zare, *Anal. Lett.*, 41 (2008) 2267.
36. S. Zhang, N. Wang, H. Yu, Y. Niu, C. Sun, *Bioelectrochemistry.*, 67 (2005) 15.
37. A. Kaushik, R. Khan, P.R. Solanki, P. Pandey, J. Alam, S. Ahmad, B. Malhotra, *Biosens. Bioelectron.*, 24 (2008) 676.
38. B. W. Lu, W. C. Chen, *J. Magn. Magn. Mater.*, 304 (2006) 400.
39. S. Deng, G. Jian, J. Lei, Z. Hu, H. Ju, *Biosens. Bioelectron.*, 25 (2009) 373.
40. J.D. Newman, A.P. Turner, *Biosens. Bioelectron.*, 20 (2005) 2435.
41. Z. Li, L. Sheng, A. Meng, C. Xie, K. Zhao, *Microchim. Acta.*, 183 (2016) 1625.

42. S. Palanisamy, C. Karuppiah, S.-M. Chen, *Colloids. Surf. B.*, 114 (2014) 164.
43. Y. Wang, H. Li, J. Kong, *Sens. Actuators. B. Chem.*, 193 (2014) 708.
44. W. Wang, Y. Xie, C. Xia, H. Du, F. Tian, *Microchim. Acta.*, 181 (2014) 1325.
45. S. Palanisamy, S. Cheemalapati, S.-M. Chen, *Mater. Sci. Eng. C.*, 34 (2014) 207.
46. M.A. Tabrizi, J.N. Varkani, *Sens. Actuators. B. Chem.*, 202 (2014) 475.
47. B. Unnikrishnan, S. Palanisamy, S.-M. Chen, *Biosens. Bioelectron.*, 39 (2013) 70.
48. F.-Y. Kong, S.-X. Gu, W.-W. Li, T.-T. Chen, Q. Xu, W. Wang, *Biosens. Bioelectron.*, 56 (2014) 77.
49. V. Mani, B. Devadas, S.-M. Chen, *Biosens. Bioelectron.*, 41 (2013) 309.
50. Q. Xu, S.-X. Gu, L. Jin, Y.-e. Zhou, Z. Yang, W. Wang, X. Hu, *Sens. Actuators. B. Chem.*, 190 (2014) 562.

© 2018 The Authors. Published by ESG (www.electrochemsci.org). This article is an open access article distributed under the terms and conditions of the Creative Commons Attribution license (<http://creativecommons.org/licenses/by/4.0/>).